Far off-shore wind energy-based hydrogen production: Technological assessment and market valuation designs

Maxime Woznicki, Guenael Le Solliec, Rodica Loisel

Far off-shore wind energy-based hydrogen production: Technological assessment and market valuation designs

Far off-shore wind energy-based hydrogen production: Technological assessment and market valuation designs

M Woznicki[1,3], G Le Solliec[1,4] and R Loisel[2,5]
[1] CEA (French Alternative Energies and Atomic Energy Commission), Nantes, France
[2] Université de Nantes, Lemna (Nantes-Atlantic Economics and Management Lab.), France

Email : [3]maxime.woznicki@cea.fr, [4]guenael.lesolliec@cea.fr, [5]rodica.loisel@univ-nantes.fr

Abstract. This article provides a techno-economic study on coupled offshore wind farm and green hydrogen production via sea water electrolysis (OWF-H_2). Offshore wind energy, wind farms (OWF) and water electrolysis (WE) technologies are described. MHyWind (the tool used to perform simulations and optimisations of such plants) is presented, as well as the models of the main components in the study. Three case studies focus on offshore wind farms, either stand-alone or connected to the grid via export cables, coupled with a battery and electrolysis systems either offshore or onshore. Exhaustive searches and optimisations performed allowed for rules of thumb to be derived on the sizing of coupled OWF-H_2 plants, that minimize costs of hydrogen production ($LCoH_2$, in €/kgH_2): Non-connected OWF-H_2, coupled to a battery, offers the lowest $LCoH_2$, without the costs of H_2 transportation, when compared to cases where the WE is installed onshore and connected to the OWF. Using a simple power distribution heuristic, increasing the number of installed WE allows the system to take advantage of more OWF energy but doesn't improve plant efficiency, whereas a battery always does. Finally, within the scope of this study, it is observed that power ratios of optimized plant architectures (leading to the lowest $LCoH_2$) are between 0.8-0.9 for P_{WE}/P_{OWF} and 0.3-0.35 for $P_{Battery}/P_{OWF}$.

1. Introduction

Global offshore wind capacity has increased from around 4 GW in 2011 to more than 22 GW in 2018, and some forecasts predict that 500 GW of installed capacity will be reached by 2050. Moreover, the coming years will see the development and deployment of cost competitive floating offshore wind technologies with turbines of more than 10 MW, unlocking tremendous wind resources available far-shore (deeper than 50 m). One of the main issues with far-shore wind resource exploitation is the grid connection, as often the cost is prohibitive. In parallel, the urgent need for alternative energy vectors to address the global warming issue and decrease Greenhouse Gas (GHG) emissions stimulates an increase in demand for clean hydrogen - either green (produced from renewable energy, via water electrolysis) or blue (produced from fossil fuels with Carbon Capture and Storage (CCS)). Hydrogen can be used for mobility, heavy transportation, industrial-sized chemistry and can even be injected into gas networks. According to DNV-GL, blue hydrogen is primarily used for heating buildings and industry while green hydrogen is used mainly for mobility purpose. In that context, it appears logical to assess the potential of coupling offshore wind farms with hydrogen production technologies (i.e. OWF-H_2) as this would make sense economically and enable mass production of green H_2 from seawater. As such, this paper represents a techno-economic study focusing on the coupling offshore wind and H_2 production.

2. Methodology

In order to assess OWF-H_2 plants, CEA, with the financial support of the French region *Pays de la Loire*, is developing a tool dedicated to techno-economic assessment of such plants: MHyWind. This programme performs simulations and optimisations of various OWF-H_2 architectures on the hour-scale by coupling offshore wind farms (OWF) with water electrolysers (WE). Various models of components from wind turbines to energy transportation can be used in simulations, such as the wind farm substation, the hydrogen compressors and storage systems, hydrogen transportation vessels, and offshore export cables. The models include parameters such as efficiency and cost functions, life expectancy and ageing. Computations can be performed on many different plant architectures, either grid-connected or off-grid, enabling the system to interact with the EPEX SPOT market and deriving fees related to local grid usage (TURPE, in France).

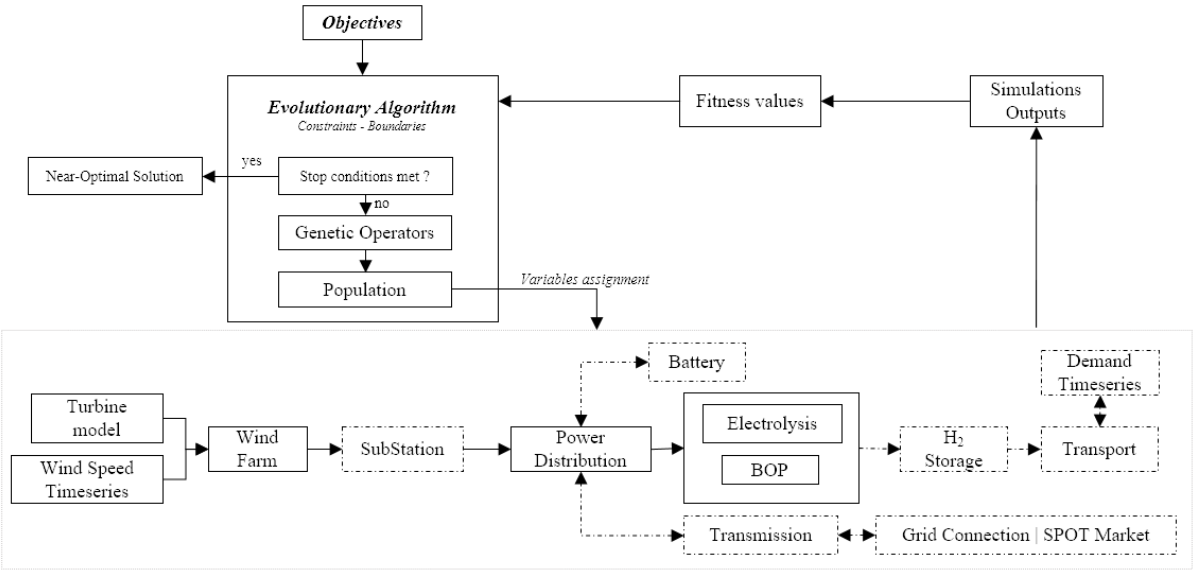

Figure 1. MHyWind General Architecture

Provided with offshore wind speed time series, and user-defined constraints like hydrogen demand time series, MHyWind performs mono and multi-objective(s) optimisation(s), using an evolutionary Genetic Algorithm [1], and finds near-optimal solutions for a number of pre-defined plant architectures, given system constraints and objectives. The main output variables which can be used in objective functions are listed in **Table 1**. Those fitness values for optimisation or analysis are mainly the levelized cost of hydrogen ($LCoH_2$), CAPEX, OPEX and various operational indicators, such as capacity factors, H_2 production volume, and wind energy losses. Depending on the plant definition to be optimized, MHyWind explores the search space by working on the design variables listed in **Table 1**. The $LCoH_2$computed is derived from the traditional LCoE (levelized Cost of Energy) formulation based on CAPEX, OPEX and hydrogen production volume, where *pl* represents the project lifetime and *r* the interest rate:

$$LCoH_2 = \frac{CAPEX + \sum_{y=1}^{pl} \frac{OPEX_y}{(1+r)^y}}{\sum_{y=1}^{pl} \frac{H2_y}{(1+r)^y}} \quad [€.kg^{-1}]$$

Table 1. Main design and output variables, for optimisations

Main design variables	Main output variables
Wind farm rated power	LCOH2
Electrolyser rated power	H2 production volume
Electrolyser technology	Electrolyser capacity factor
Number of electrolysers	Total CAPEX
Hydrogen storage capacity	Total OPEX
Transport capacity	Energy Loss

Battery capacity	Unmet demand
Export cable capacity	Total Revenues
Turbine power curve	
Battery enabled	
Grid connection enabled	
Purchase elec. from the grid	
Sell elec. to the grid	
Electricity sale price threshold	
Grid power subscription	

2.1. Offshore Wind Farm

An offshore wind farm [2], is composed of several wind turbines, with their associated rated power and power curve. All turbines are connected via inner-array cables to an electrical sub-station, whose function is to step up the voltage and thereby minimize transmission losses through one or more export cables transporting the energy to shore. Offshore wind farms can be either bottom fixed (typically used down to depths of 50 m where the supporting structure of turbines are directly installed in the seabed (monopile, jacket, or tripod)) or floating wind farms - installed in water deeper than 50 m, with the floating structures (tension leg platforms, semi-submersible platforms, spar) moored and anchored to the seabed.

The power output of the wind farm at substation level P_{owf} is a directly computed function of the number of turbines N_T , local wind speed time series $U_{HH}(t)$ (with a correction factor allowing to derive the wind speed at hub height) and turbine power curve $P_{turbine}$.

2.2. Wind turbine

The power output of a wind turbine is directly derived from wind kinetic power and a power coefficient C_p depending on turbine design and wind speed [3]. Wind turbines are designed to operate with an increasing C_p from a cut-in wind speed U_{ci} (~4 m.s^{-1}) to the rated wind speed U_{rated} (~12 m.s^{-1}).

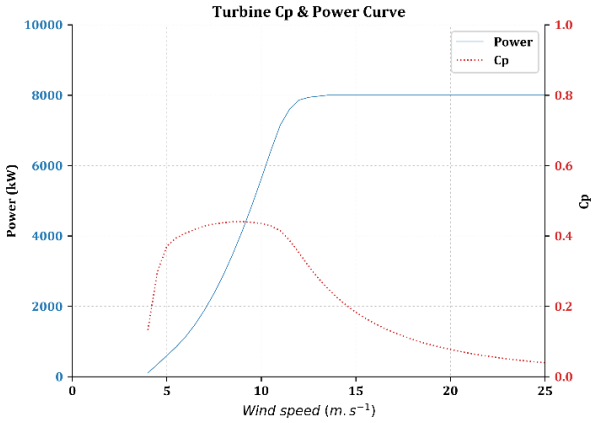

Figure 2. Leanwind 8MW Reference Turbine *Cp* and power curves

When the turbine rated power is reached, pitch control takes over, inducing blade stall and decreasing C_p , ensuring constant rated power $P_{turbine}^{rated}$ until the cut-out wind speed U_{co} (~25 m.s^{-1}). The wind farm rated power, and analytic turbine power curves can be used as design variables.

2.3. Water Electrolysis

Water electrolysis (WE) is the electrochemical process of splitting water into hydrogen and oxygen by supplying electrical and thermal energy. This can be performed using various electrolysis technologies such as: alkaline electrolysis (AEC, which has been used commercially for decades and uses an aqueous KOH solution), proton exchange membrane electrolysis (PEMEC, which has been commercialized more recently and shows promise with its power density and dynamic performance), and solid oxide electrolysis (SOEC) also known as high temperature electrolysis. SOEC technology, which is close to the commercial stage, can use waste heat to increase efficiency and to decrease electrical consumption.

Each of these aforementioned technologies has its own benefits and drawbacks in terms of operating temperature and pressure, output gas pressure, cold and warm start duration, gas purity, life expectancy and working range (these are depicted in **Table 2**). Detailed descriptions of the various electrolysis technologies are available in [4], and the future of water electrolysis technologies in terms of performance and costs is outlined in [5].

Table 2.Summary of parameters across state-of-the-art water electrolysis technologies

	AEC	PEMEC	SOEC
Cell temperature (°C)	60 - 90	50 - 80	700 – 900
Typical pressure (bar)	10 -30	20 - 50	1 – 15
Current density (A/cm²)	0.25 – 0.45	1 - 2	0.3 – 1
Cell area (m²)	<3.6	<0.13	<0.06
Working range (% nominal load)	20-100	0-100	-100/+100
Cold start-up time	1-2 h	5-10 min	Hours
Warm start-up time	1-5 mins	< 10 s	15 min
Lifetime (kh)	55-120	60-100	8-20
Efficiency degradation (%/a)	0.25–1.5	0.5–2.5	3–50

Electrolyser is modelled using an analytic formulation of its efficiency η depending on the load and calibrated with a degradation factor *a(t)* to simulate ageing. Hydrogen flow rate is then directly computed from electrical power consumption and its efficiency as follows:

$$\dot{m}_{H2} = \frac{P_{WE}^{in}(t).\left(\eta\left(\frac{P_{WE}^{in}(t)}{P_{WE}^{rated}}\right) - a(t)\right)}{LHV_{H2}}, with\ P_{WE}^{in,min} \leq P_{WE}^{in}(t) \leq P_{WE}^{rated}$$

$$\dot{m}_{H2} = \frac{P_{WE}^{rated}.\left(\eta(1) - a(t)\right)}{LHV_{H2}}, when\ P_{WE}^{rated} \leq P^{av}$$

$$\dot{m}_{H2} = 0, when\ P^{av} < P_{WE}^{in,min}$$

With P^{av} being the available input power from an OWF and/or battery, for example.

The electrolysis rated power, the number of electrolysers, and electrolyser technology can be used as design variables. For the moment, the cold and warm start-up behaviours are not modelled.

2.4.Hydrogen compression and storage

According to [9], the required energy E_{comp}, to compress 1 kg of H_2 from output pressure p_0 to storage pressure p_f, is derived from **Figure 3**. Compressor rated power is then inferred from the maximum hydrogen flow rate of the electrolysis system:

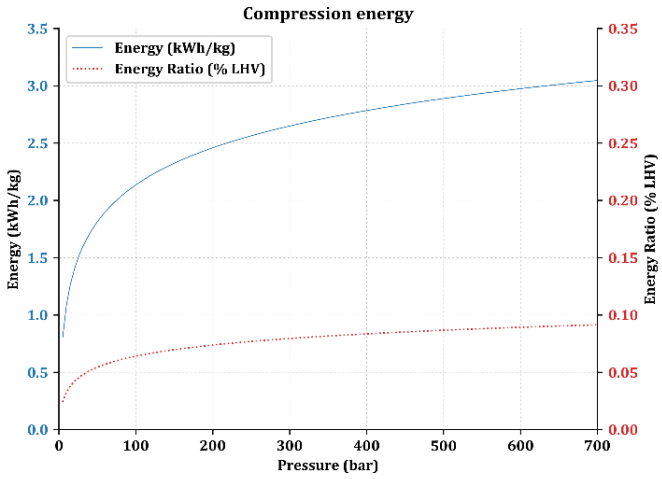

Figure 3. Hydrogen Compression - Energy Requirements

The hydrogen storage is modelled using a capacity parameter which can be used as a design variable.

2.5. Hydrogen transportation

Hydrogen transportation with vessels has been implemented. Transportation can be triggered in two ways: either the vessel arrives at the right time (just before offshore hydrogen storage is full) or a frequency of visit can be defined. Transportation costs are then computed based on vessels' daily rate, cost of fuel, distance to shore and carrying capacity. The vessel capacity can be used as a design variable.

2.6. Battery

Battery rated power is computed with a fixed C-rate parameter and a capacity as a design variable. State of charge, efficiency loss and life expectancy are modelled based on the following parameters: charge and discharge efficiency, depth of discharge, life expectancy in number of cycles and efficiency loss over time. When needed, replacement costs are added to the project OPEX.

2.7. Grid connection and offshore export cable

Plants can be connected to the grid to study the impact of energy exchange: sale or purchase of electricity on the EPEX SPOT market and assessment of fees (TURPE [14]) applied when using the national electricity transport network (RTE in France). Offshore export cables will have a constant efficiency. More advanced models, such as those described by [11] and [12], can also be implemented. In order to study the impact of cable sizing, several sizes can be tested during optimisations, with their associated cost functions, provided by [13]. The export cable models, capacity and the usage strategy of the grid (power subscription, sale, purchase, and price thresholds) can be used as design variables.

2.8. Power balancing

MHyWind balances power depending on components available in the system and their power/energy capabilities at any timestep t, with the aim of providing as much power as possible to the hydrogen production plant ($P_{H2}^{in} = P_{battery} + P_{owf}$) within its working range. When available power from the wind farm is out the power range of the H_2 production plant, power is firstly used to charge the battery. If the battery is charged, the remaining power is sent to the grid (if the plant is connected to the grid) otherwise energy is lost. Different power distribution strategies can be implemented to assess power distribution and can be used as a design variable for optimisation.

3. Case studies

3.1. Definition

Using the capabilities of MHyWind, the following three scenarios (whose parameters and boundaries are listed in **Table 3**) were studied, producing hydrogen compressed to 350 bar:

1) A **non-connected** offshore wind farm, coupled **offshore** with a battery and an electrolysis system,
2) An offshore wind farm, **connected** to the grid via an export cable, coupled **offshore** with a battery and an electrolysis system,
3) An offshore wind farm, **connected** to the grid via an export cable, coupled **onshore** with a battery and an electrolysis system.

The primary aim is to understand the influence of several optimisation variables such as battery capacity, total electrolysis power, number of electrolysers and the capability of the plant to sell energy to the grid. If the OWF is not connected to the grid, a fraction of the power generated may be discarded because the WE system only operates within a defined range, meaning that input power above or below the range limits cannot be used. As such, WE systems were coupled with batteries to minimize energy losses by increasing the OWF power range that could be absorbed and assessing the outcome. Moreover, as WE

efficiency is function of the load, the modularity offered by this kind of design is of interest, as it may minimise ageing of electrolysers. For connected cases, electricity is only sold (at EPEX SPOT market price) when the battery (if installed) is full, or wind farm power output is out of the working range of the electrolysis system.

Table 3. Case study parameters & boundaries

Case study ID	CS1	CS2	CS3
Project Life (y) / Interest Rate (%)	15 / 7	15 / 7	15 / 7
Wind farm location	Offshore	Offshore	Offshore
Hydrogen Production	Offshore	Offshore	Onshore
Grid connection / Export Cable	No	Yes	Yes
Hydrogen Output Pressure	350 bar	350 bar	350 bar
Turbine power (MW)	4.2	4.2	4.2
Number of turbines	50-100	50-100	50-100
Turbine capex - €/kW [10]	2880	2880	2880
P_{we} **(MW)**	[0.1-1].P_{owf}	[0.1-1].P_{owf}	[0.1-1].P_{owf}
Battery Capacity (MWh)	10-200	10-200	10-200
# Electrolysers	1-5	1-5	1-5
Export Cable Capacity (MVA)	-	[0.1-1].P_{owf}	P_{owf}
Electrolysers installation costs ratio	3	3	1
Compressor efficiency	0.7	0.7	0.7
Export cable efficiency	0.96	0.96	0.96

3.2. Parameters

3.2.1. Turbine power output model – The turbine power curve was fitted using a 6 parameter logistic function [6], $U_{HH}(z)$ being the corrected wind speed at hub height (z), using Davenport's power law, and a power coefficient α depending on the type of terrain where the wind farm is located ($\alpha = 0.11$ for offshore):

$$P_T(U_{HH}) = \delta + \frac{\alpha-\delta}{(\varepsilon+e^{(-\beta.(U_{HH}-v_0))})^{\frac{1}{\gamma}}} \ , \ U_{HH}(z) = U_{z_0}.(\frac{z}{z_0})^{\alpha}$$

Table 4. Power Curve parameters

Turbine	α	β	δ	ε	γ	v_0	U_{ci}	U_{co}	Hub Height
MHI-Vestas 4.2 MW	2872.82	4.53	-671.28	0.00196	19.670	9.846	3	25	94

Wake effect is not accounted for within the simulated wind farms. Wind speed timeseries were taken around 70 km offshore Saint-Nazaire, France on soda-pro.com [15].

3.2.2. Water electrolysers -**Figure 4**, **Figure 5** and **Table 5** present two efficiency models rebuilt based on [7] for Alkaline electrolysers and on a manufacturer's efficiency curve for PEM electrolysers (rectifier included). CAPEX functions have been fitted based on [8] and [5].

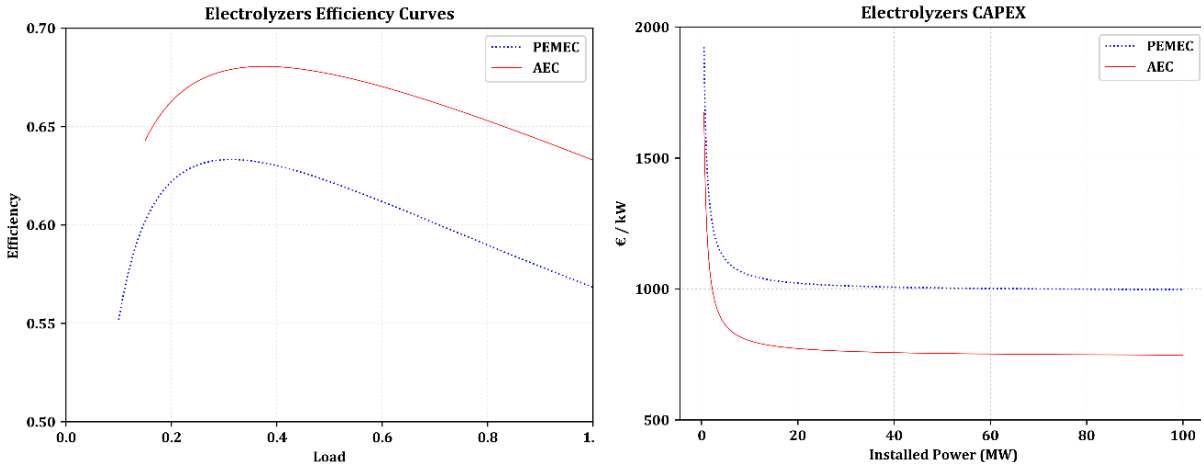

Figure 4. Electrolyser Efficiency Curves

Figure 5. Electrolyser CAPEX Functions

Due to the lack of existing data, electrolyser installation costs have been based on assumptions made by BVGAssociates [2] and considered equivalent to substation installation costs, at 41 €/kW for offshore cases, and 14 €/kW, for onshore cases (less complex, require no onshore cable installation).

Table 5. Electrolyser model properties

	AEC	PEMEC
Working range (% load)	15-100	10-100
Lifetime (kh)	60	50
Eff. degradation (%/y)	0.01	0.015

Table 6. Battery Model Parameters

Battery parameters	**Value**
C-rate	2
Charge efficiency - $\eta_{charge}(load)$	0.9
Discharge efficiency - $\eta_{discharge}(load)$	0.95
Depth of discharge (% capacity)	0.8
Life expectancy (# of cycles)	3000
Efficiency loss over lifetime (%)	0.1

3.2.3. Battery Model - **Table 6** outlines the parameters used for the case studies reported in this paper, with the associated acquisition cost function [10] depicted in **Figure 6**.

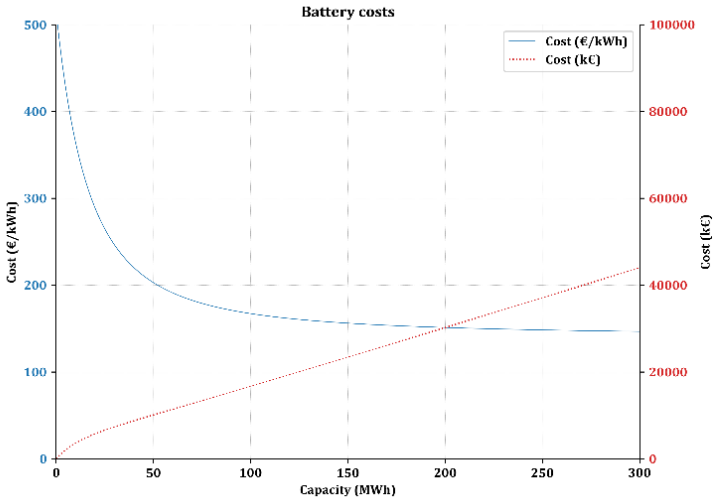

Figure 6. Battery Cost function

4. **Results and discussion**

The results of optimisation for the three case studies with the objective of minimizing the LCoH2 are presented in **Table 7**, while sensitivity analysis of the function of battery sizing and power factor is presented in **Figure 7**.

It is immediately noticeable that AEC technology always outperforms PEMEC, due to its lower costs and higher efficiency despite its wider working range. Wind farm power reaches its upper limit (420 MW) because of the absence of constraints on hydrogen demand, which was expected considering CAPEX decrease function of power. It can be observed that in all cases, optimally sized OWF-H_2 plants tend to minimize energy losses to improve the $LCoH_2$ with very close power factors: the optimal power ratio between electrolyser and wind farm is 0.8 - 0.9 and optimal power ratio between battery and wind farm should be within 0.3 – 0.35. Other simulations confirm those orders of magnitude, independent of the wind farm capacity, which is mainly due to the assumption of power balancing which prioritizes H_2 production over the sale of electricity. The top-left graph in **Figure 7** shows that H_2 production volume saturates once optimal battery size is reached, negating energy loss when OWF power is lower than the minimum power required for WE. Beyond this optimal sizing, an increasing power capacity degrades production costs performances.

The results also show that installing several electrolysers does not appear to benefit system optimisation. This can be explained due to the sequential operation of the electrolyser management strategy used in these case studies, which does not aim for an optimal power distribution between electrolysers. This aspect of the study will be the subject of future work to develop an optimal, high-level control strategy for the entire WE system (number of electrolysers, unitary power and power distribution) which will improve overall efficiency while minimizing the ageing of electrolysers and, consequently, the OPEX.

H_2 is produced offshore in both cases CS1 and CS2, and as such, $LCoH_2$ results for both studies can be compared. This comparison shows that when H_2 production is prioritized over the sale of electricity, with an optimally sized system, energy transmitted to the grid is minimized, and electricity sale income does not improve (i.e. lower) the $LCoH_2$. Conversely, when power is insufficiently high for WE, the trend is reversed, and the amount of electricity transmitted to the grid increases. The additional income from the sale of electricity limits $LCoH_2$ variations for CS2, whereas energy is lost for CS1, and $LCoH_2$ variations are more distinct. As such, in a hypothetical scenario constrained by a demand for high production of electricity, CS2 may represent a more efficient setup. It may also therefore be more productive to consider stand-alone wind farms (such as the setup for CS1) for offshore production of hydrogen.

Table 7. Optimisation results of case studies

	CS1	**CS2**	**CS3**
Wind Farm Power (MW)	420	420	420
WE technology	AEC	AEC	AEC
Electrolyser Power (MW)	374	370	361
Number of electrolysers	1	1	1
Power Ratio (WE/OWF)	0.89	0.88	0.86
WE Capacity Factor	0.479	0.483	0.487
Battery Capacity (MWh)	71	65	61
Battery Power (MW)	142	130	122
Export Cable Capacity (MVA)	-	1x91.7MVA	2x290MVA
Energy transmitted to grid	-	0.3%	0.9%
$LCoH_2$ (€/kgH_2)	**6.88**	**7.067**	**7.394**
H_2 Production (tons)	458372	456332	445929
Energy Loss (% OWF output)	0.02%	0%	0%

As shown in the bottom-right graph of **Figure 7**, hydrogen production in CS3 is lower than both CS1 and CS2. Indeed, H_2 yields are higher when production is done offshore, as power provided to the electrolysis system does not suffer from the financial costs and energy losses associated with transmission. However, H_2 produced in CS3 would be available onshore whereas H_2 would still need to be transported to shore for CS1 and CS2. Factoring in the associated transportation costs for CS1, the $LCoH_2$ would increase by 7.9% to 7.45 €/kg, with the following assumptions being made: vessel capacity of 20 tons, a daily rate of 14 k€, and fuel price of 0.6 €/L.

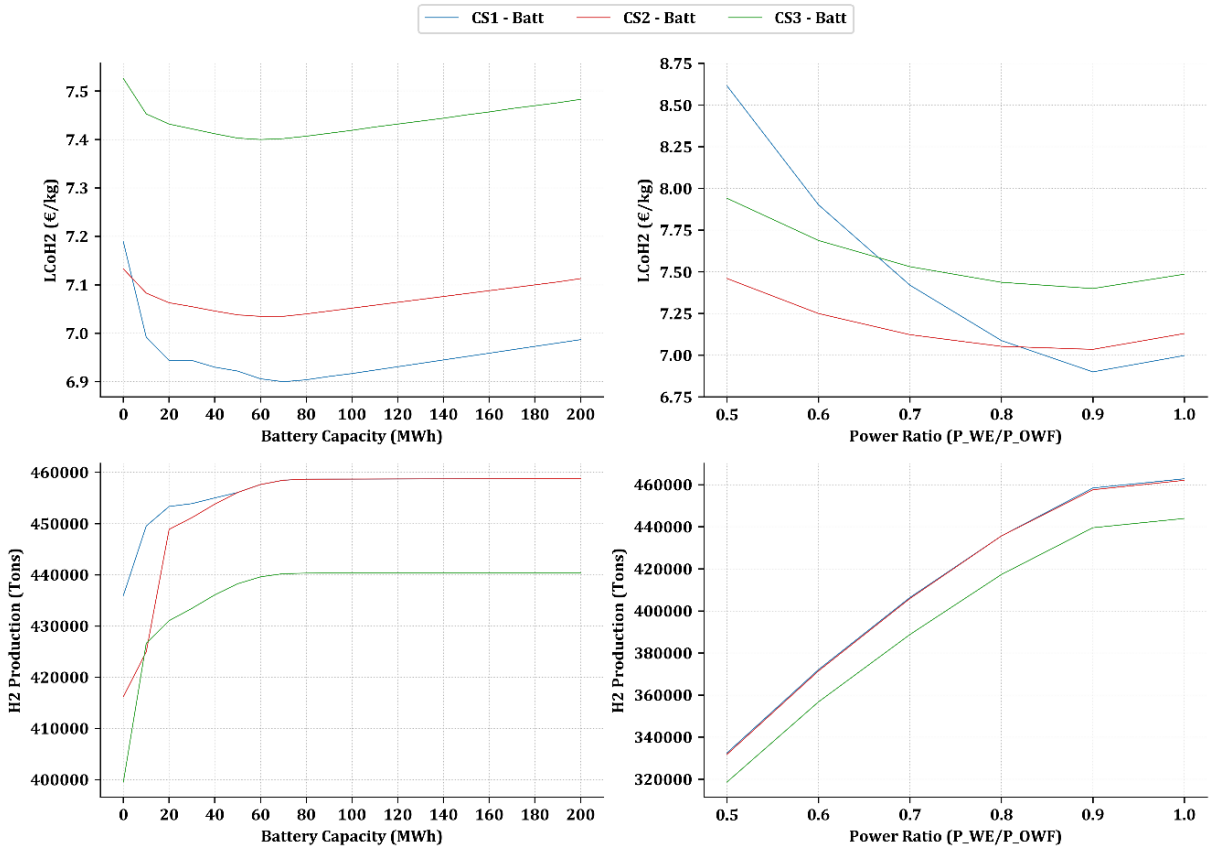

Figure 7. Sensitivity analysis of case studies, with 420 MW of Wind Farm Power

5. **Conclusion**

Although a number of variables such as exact project setup and installation costs could not be considered in this study, and despite a limited knowledge of the integration constraints at sea being used in simulations, the results obtained suggest that it should be possible to achieve offshore production of hydrogen at an economically viable level in the medium-term.

Furthermore, some aspects not considered in this study, such as the effect of other design parameters and optimized power distribution strategies, need to be assessed and could potentially lead to better plant architecture and performance improvements in the future. These considerations include:

- Integration of electrolyser start-up times into simulations,
- Testing of turbine electrical generator downsizing, decreasing power output, varying the associated costs of turbines, substation and energy transmission,
- Formulating a high-level power distribution strategy based on battery usage, electrolysis load, hydrogen production volume, electricity purchase costs and electricity sale revenues to identify optimal trade-offs in power use, at each time-step, using detailed knowledge of OWF power output and up to date (12 – 24 hrs) SPOT market prices,
- Applying thresholds on the sale/purchase prices on the SPOT market and investigating the effect this may have on the performance of production plants.

References

[1] E. Elbeltagia, T. Hegazyb and D. Griersonb, "Comparison among five evolutionary-based optimization algorithms," *Advanced Engineering Informatics*, pp. 43-53, 2005.

[2] BVG Associates, Guide to an offshore wind farm, 2019.

[3] C. Desmond, J. Murphy, L. Blonk and W. Haans, "Description of an 8 MW reference wind turbine," *Journal of Physics,* vol. Conference Series 753, 2016.

[4] A. Buttler and H. Spliethoff, "Current status of water electrolysis for energy storage, grid balancing and sector coupling via power-to-gas and power-to-liquids: A review," *Renewable and Sustainable Energy Reviews,* 2017.

[5] O. Schmidt, A. Gambhir, I. Staffell, A. Hawkes, J. Nelson and S. Few, "Future cost and performance of water electrolysis: An expert elicitation study," *International Journal of Hydrogen Energy,* 2017.

[6] RTE, "TURPE 5 - Tarification des réseaux, édition Juillet 2018," 2018.

[7] S. Gasnier, A. André, S. Poullain, V. Debusschere, B. Francois and P. Egrot, "Models of AC and DC Cable Systems for Technical and Economic Evaluation of Offshore Wind Farm Connection," *International Journal of Electrical Energy,* 2018.

[8] H. Brakelmann, "Loss Determination for Long Three-Phase High-Voltage Submarine Cables," 2003.

[9] DTOcean Project, "Deliverable 3.4: Prediction of reliability and economics of the offshore electrical infrastructure with recommendations and guidelines for the environmental impacts of the proposed array configurations," 2015.

[10] M. Noonan, T. Stehly, D. Mora, L. Kitzing, G. Smart, V. Berkhout and Y. Kikuchi, "IEA Wind TCP Task 26: Offshore Wind Energy International Comparative Analysis," 2018.

[11] D. Villanueva and A. Feijóo, "Comparison of logistic functions for modeling wind turbine power curves," *Electric Power Systems Research,* 2017.

[12] MINES ParisTech, "Soda-Pro - MERRA-2 RE-ANALYSIS," [Online]. Available: http://www.soda-pro.com/web-services/meteo-data/merra.

[13] F. J. Pino, L. Valverde and F. Rosa, "Influence of wind turbine power curve and electrolyzer operating temperature on hydrogen production in wind–hydrogen systems," *Journal of Power Sources,* 2010.

[14] S. M. Saba, M. Müller, M. Robinius and D. Stolten, "The investment costs of electrolysis - A comparison of cost studies from the past 30 years," *International Journal of Hydrogen Energy,* 2017.

[15] NREL, " U.S. Utility-Scale PhotovoltaicsPlus-Energy Storage System Costs Benchmark," 2018.

[16] U. Eberle, M. Felderhoff and F. Schüth, "Chemical and Physical Solutions for Hydrogen Storage," *Angewandte Chemie International,* 2009.